ACS APPLIED MATERIALS & INTERFACES

Research Article

www.acsami.org

Dual Effective Organic/Inorganic Hybrid Star-Shaped Polymer Coatings on Ultrafiltration Membrane for Bio- and Oil-Fouling Resistance

Dong-Gyun Kim,[†,‡] Hyo Kang,*[,†,§] Sungsoo Han,[§] and Jong-Chan Lee*[,‡]

[‡]School of Chemical and Biological Engineering and Institute of Chemical Process, Seoul National University, 599 Gwanak-ro, Gwanak-gu, Seoul 151-742, Republic of Korea

[§]Energy Lab., Samsung Advanced Institute of Technology, Samsung Electronics Co., Ltd., Nongseo-dong, Giheung-gu, Gyeonggi-do 446-712, Republic of Korea

Supporting Information

ABSTRACT: Amphiphilic organic/inorganic hybrid star-shaped polymers (SPP) were prepared by atom transfer radical polymerization (ATRP) using poly(ethylene glycol) methyl ether methacrylate (PEGMA) and 3-(3,5,7,9,11,13,15-heptacyclohexyl-pentacyclo[9.5.1.1^{3,9}.1^{5,15}.1^{7,13}]-octasiloxane-1-yl)propyl methacrylate (MA-POSS) as monomers and octakis(2-bromo-2-methylpropionoxypropyldimethylsiloxy)-octasilsesquioxane (OBPS) as an initiator. Star-shaped polymers (SPM) having PEGMA and methyl methacrylate (MMA) moieties were also prepared for comparative purposes. Polysulfone (PSf) ultrafiltration membranes coated with the SPP showed higher bio- and oil-fouling resistance and flux-recovery ability than the bare PSf membrane. Moreover, the SPP-coated membranes exhibited better antifouling properties than the SPM-coated membrane when they were used for oil/water emulsion filtration. The dual effective antifouling properties of the SPP were ascribed to the simultaneous enrichment of hydrophilic PEG and hydrophobic POSS moieties on the membrane surfaces resulting in the decrease in interactions with proteins and the increase in repellence to oils.

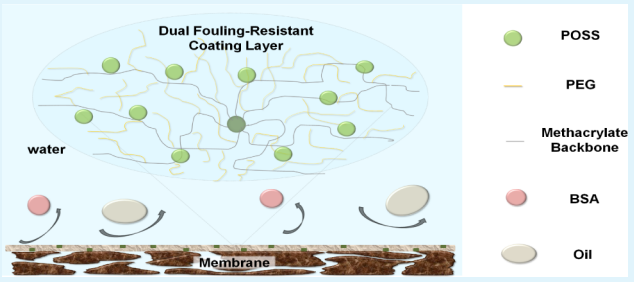

KEYWORDS: *surface modification, organic/inorganic hybrid materials, star-shaped polymers, membranes, antifouling*

INTRODUCTION

Membrane filtration has been widely used in environmental and biochemical applications.[1,2] Substances in water such as proteins and oils generate membrane fouling that causes a decrease in water permeation flux followed by a subsequent increase in energy demand for filtration.[3−5] As the membrane fouling is caused by interactions between the membrane surface and foulants, it is essential to modify the membrane surface to reduce fouling. Many studies have been conducted regarding membrane surface modifications to reduce biofouling by introducing hydrophilic moieties such as poly(ethylene glycol) (PEG) on the surfaces.[6−14] However, there have been many fewer studies concerning the surface modification for oil-fouling resistance, even though large quantities of wastewater that contain large amounts of oils are generated by various industries.[15−17] Although most studies on oil-fouling resistant membranes have demonstrated that imparting hydrophilicity to the membrane surfaces results in an increase in oil-fouling resistant properties, the permeation flux of the membranes still decreases significantly in a short period of time.[16−20] Recently, amphiphilic membrane surfaces, consisting of hydrophilic PEG segments and hydrophobic fluoropolymer segments, were studied to suppress the flux-decline during oil/water emulsion filtration.[21,22]

Polyhedral oligomeric silsesquioxane (POSS) has attracted considerable interest because of its well-defined nanoscale organic/inorganic hybrid structure.[23] POSS-based hybrid materials show enhanced thermal stability and mechanical properties due to molecular level dispersion of POSS in the polymers.[24−27] Recent investigations have demonstrated that POSS materials also hold promise as surface modifiers.[28−34] In particular, oleophobic surfaces have been prepared using POSS derivatives with low surface energy originating from its unique chemical structure of the silicon−oxygen core with organic groups attached to each silicon atom.[30−34] Thus, it might be possible to prepare amphiphilic coating materials with bio- and oil-fouling resistance and fouling release properties by combining oleophobic POSS and hydrophilic PEG derivatives.

Star-shaped polymers exhibit unique physical properties and morphologies that are not observed in their corresponding linear polymers.[35,36] Structurally, they have a number of linear

Received: August 2, 2012
Accepted: October 10, 2012
Published: October 10, 2012

   dx.doi.org/10.1021/am301538h | ACS Appl. Mater. Interfaces 2012, 4, 5898−5906

Table 1. Results of the Synthesis of the Star-Shaped Polymers from Different Co-Monomer Feeding Ratios

	composition (PEGMA: MA-POSS or MMA)[a]						
sample	feed (mol %)	in polymer (mol %)	in polymer (wt %)	M_n[b] ($\times 10^{-3}$, RI)	M_n[c] ($\times 10^{-3}$, MALLS)	PDI[b] [c]	solubility[d] in H_2O/MeOH
SPP100	100:0	100:0	100:0	53.5	267.1	1.25 (1.24)	S/S
SPP87	92:8	94:6	87:13	35.4	410.5	1.27 (1.16)	I/S
SPP74	81:19	87:13	74:26	42.7	179.5	1.21 (1.07)	I/S
SPP57	65:35	76:24	57:43	37.2	116.8	1.21 (1.15)	I/I
SPM69	37:63	32:68	69:31	29.2	51.0	1.21 (1.20)	S/S
SPM46	18:82	15:85	46:54	28.2	47.3	1.24 (1.19)	I/S
SPM26	9:91	7:93	26:74	23.2	34.7	1.29 (1.23)	I/I

[a]Determined by ^{1}H NMR. [b]Determined by GPC using refractive index (RI) detector, calibrated with linear polystyrene standards (THF). [c]Determined by GPC using multiangle laser light scattering (MALLS) detector (THF). [d]S = soluble, I = insoluble.

polymeric arms that emerge out of a central core, which increase polymer segment density compared to linear polymers, and the end groups of the arms are located at the periphery of the molecules due to steric restrictions toward the center of the stars.[37] In our recent study, antifouling coating layers on PSf ultrafiltration membranes were prepared from star-shaped polymers with poly(ethylene glycol) methyl ether methacrylate (PEGMA) and methyl methacrylate (MMA) moieties.[38] These membranes exhibited higher biofouling resistance and flux-recovery ability than those coated with the corresponding linear polymers. Therefore, the star-shaped architecture further enhances the antifouling properties of the coating materials when applied to the membrane surface.

In this study, we designed organic/inorganic hybrid star-shaped polymers (SPP) as antifouling coating materials containing poly(poly(ethylene glycol) methyl ether methacrylate) (PPEGMA) segments for bio- and oil-fouling resistance and poly(3-(3,5,7,9,11,13,15-heptacyclohexyl-pentacyclo-[9.5.1.1^{3,9}.1^{5,15}.1^{7,13}]-octasiloxane-1-yl)propyl methacrylate) (P(MA-POSS)) segments for oil-repellency and coating stability. The fouling behavior of the SPP-coated PSf membranes was investigated and compared with that of membranes coated with a star-shaped polymer (SPM) having poly(methyl methacrylate) (PMMA) and PPEGMA segments and the bare PSf membrane by employing bovine serum albumin (BSA) and vacuum pump oil as representative bio- and oil-foulants, respectively. The discussion mainly focuses on the correlation between the surface composition and fouling-resistant ability of the membranes. In comparison to SPM-coated membrane, the SPP-coated membranes showed similar flux-decline resistance and flux-recovery ability for filtering the BSA solution and largely enhanced the flux properties for oil/water emulsion filtration.

EXPERIMENTAL SECTION

Materials. Copper(I) bromide (CuBr, 98%), *N,N,N′,N′,N″*-pentamethyldiethylenetriamine (PMDETA, 99%), bovine serum albumin (BSA, M_w = 67 kDa), phosphate buffer saline (PBS, pH 7.4), sodium dodecylsulfate (SDS, > 99%), all from Aldrich, were used as received. Dodecyltrichlorosilane (>97%) was purchased from TCI and used as received. Octakis(2-bromo-2-methylpropionoxy-propyldimethylsiloxy)silsesquioxane (OBPS) was synthesized similarly with the route described elsewhere (see the detailed procedure in Supporting Information).[39] Methacryl-Cyclohexyl-POSS (3-(3,5,7,9,11,13,15-heptacyclohexyl-pentacyclo[9.5.1.1^{3,9}.1^{5,15}.1^{7,13}]-octasiloxane-1-yl)propyl methacrylate, MA-POSS) was obtained from Hybrid Plastics Inc. and used as received. Poly(ethylene glycol) methyl ether methacrylate (PEGMA, average M_n = 475, Aldrich) was passed through a column filled with neutral alumina to remove the inhibitor before use. Vacuum pump oil (SMR-100) was obtained from Ulvac Kiko Inc. Toluene was distilled over calcium hydride. All other reagents and solvents were used as received from standard vendors.

Synthesis of Organic/Inorganic Hybrid Star-Shaped Polymers. The abbreviation of star-shaped polymers containing PEGMA and MA-POSS monomeric units is SPP. The following procedure was used for the preparation of SPP74 containing 74 wt % of PEGMA monomeric units. OBPS (46 mg, 0.017 mmol), PEGMA (5.3 g, 11 mmol), MA-POSS (2.9 g, 2.6 mmol), and toluene (20 mL) were placed into a 100 mL Schlenk flask equipped with a magnetic stirring bar and the mixture was deoxygenated by three freeze−pump−thaw cycles. After CuBr (10 mg, 0.069 mmol) was introduced to the flask under the protection of N_2 flow, the flask was subjected to two more freeze−pump−thaw cycles and backfilled with N_2 to restore atmospheric pressure and maintain an inert environment. Then the flask was placed into an oil bath thermostatted at 65 °C. Finally, PMDETA (15 μL, 0.069 mmol) was injected into the reaction flask to initiate polymerization. After 6 h of polymerization, the solution was exposed to the air. The mixture was diluted with dichloromethane and passed through a neutral alumina column to remove copper catalysts. After removing most of the solvent, the solution was precipitated into an excess of hexane. The dissolution−precipitation procedure was repeated for three times, yielding a white mass (2.4 g). The monomer conversion was determined by ^{1}H NMR to be 42% and 26% for PEGMA and MA-POSS, respectively. Other SPPs were prepared using the same procedure except the monomer feed ratio (PEGMA:MA-POSS) as shown in Table 1. ^{1}H NMR (300 MHz, $CDCl_3$, δ/ppm, TMS ref) of SPP74: 4.1 (CH_2−O−C(O)), 3.5−3.9 (CH_2−CH_2−O), 3.41 (CH_3−O), 1.73 (cyclohexyl, CH_2), 1.24 (cyclohexyl, CH_2), 0.76 (cyclohexyl, C*H*), 0.7−2 (methacrylate backbone, CH_2−C(CH_3)(C═O)).

Preparation of Star-Shaped Polymer-Coated Membranes. Polysulfone (PSf) ultrafiltration membrane (SePRO) was activated in methanol (MeOH) for 10 min and used as a support for the antifouling polymer coatings. The star-shaped polymers were dissolved in MeOH to prepare 1 wt % membrane coating solutions. The PSf membranes were coated using the solutions by spin-coating method (1000 rpm, 60 s) and air-dried.

Membrane Filtration Experiments. Filtration experiments were conducted on 76 mm diameter membranes using stirred, dead-end filtration cell (Amicon 8400) having an effective filtration area of 41.8 cm^2. The feed side of the system was pressed under 1 bar by nitrogen gas and all the experiments were carried out at an agitating speed of 200 rpm and room temperature. The pure water flux J_{w1} (L $(m^2h)^{-1}$, LMH) was obtained from the volume of the permeated water within 1 h. For the fouling resistance test, BSA phosphate buffer solution (1 g L^{-1}, pH 7.0) or oil/water emulsion (0.9 g L^{-1} for oil and 0.1 g L^{-1} for SDS) were forced to permeate through the membrane at the same pressure, and the flux at each time was recorded as J_p. To analyze the flux-recovery ability of the membranes, we cleaned the membranes by sonication in a bath filled with deionized water (Milli-Q purity) for 10 min after the filtration experiments of 30, 60, 120, and 180 min, and then measured water fluxes again with the cleaned membranes. All the filtration experiments for each sample were performed more than three times to confirm the reproducibility.

Scheme 1. Synthesis of Star-Shaped Antifouling Coating Materials ((a) SPP and (b) SPM) via Atom Transfer Radical Polymerization Using Octafunctional Silsesquioxane (OBPS) as Initiator

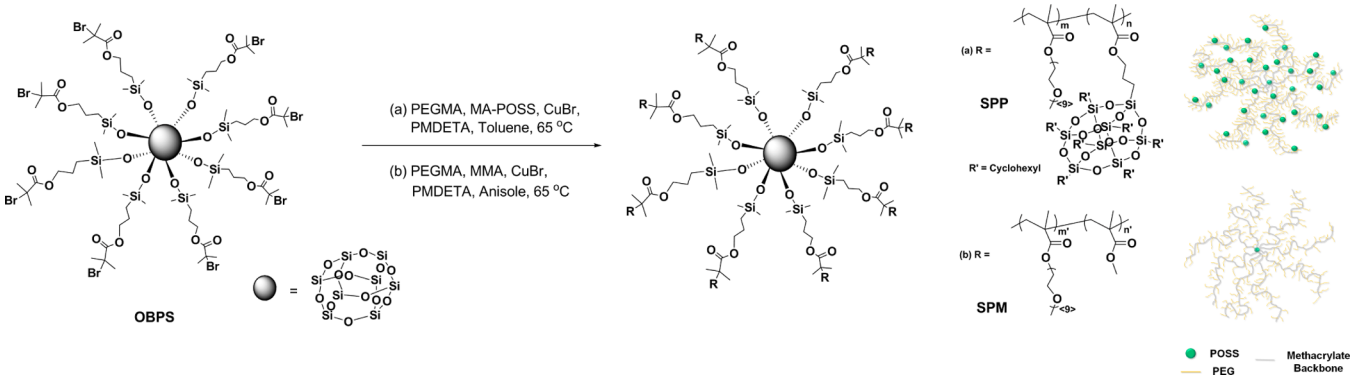

Characterization. ^{1}H nuclear magnetic resonance (NMR) spectra were recorded on a JEOL JNM LA-300 spectrometer in $CDCl_3$. Molecular weight (M_n, M_w) and polydispersity index (PDI) were analyzed by gel permeation chromatography (GPC). Relative molecular weight measurements were carried out using a Waters 515 HPLC pump equipped with three columns including PLgel 5.0 μm guard, MIXED-C, and MIXED-D from Polymer Laboratories at 35 °C in series with a Viscotec T60A refractive index (RI) detector. The system with a RI detector was calibrated using polystyrene standards from Polymer Laboratories. GPC with multiangle laser light scattering (MALLS) detector for the analysis of the absolute molecular weight of polymers was performed using a Waters 515 HPLC pump equipped with three columns including PLgel 5.0 μm guard, MIXED-C, and MIXED-D from Polymer Laboratories at 35 °C in series with a Wyatt Technology MiniDAWN^{TM} triple-angle laser light scattering detector and a Wyatt Technology Optilab DSP interferometric refractometer. HPLC grade THF (J. T. Baker) was used as an eluent at a flow rate of 1.0 mL min^{-1}. Contact angles from decane captive bubble in water were measured by a Krüss DSA10 contact angle analyzer interfaced to a computer running drop shape analysis software. The contact angles for each sample were measured a minimum of five times on three independently prepared membranes. The surface composition of the membranes was analyzed by X-ray photoelectron spectroscopy (XPS, PHI-1600) using Mg Kα (1254.0 eV) as the radiation source. Survey spectra were collected over a range of 0−1100 eV, followed by high resolution scan of the C 1s, O 1s, S 2p, and Si 2p regions. Interaction forces between the polymer-coated surface and BSA- or dodecyl-tethered tips were measured by atomic force microscope (AFM, Seiko Instrument, SPA-400, Japan). A BSA-tethered silicon cantilever was prepared according to the procedure described elsewhere.[38,40] To prepare a dodecyl-tethered AFM tip, the silicon cantilever (Nanosensors, CONTR) was treated with oxygen plasma (150 W, 30 s) and then chemically modified by dodecyltrichlorosilane toluene solution (10 mM) for 2 h. After being washed by toluene, and subsequently by ethanol several times, the tip was air-dried. We used a spring constant of 0.2 N m^{-1}, supplied by the manufacturer. A speed of 0.1 μm s^{-1} was applied to obtain the force−extension curve during approach and retraction of the polymer-coated surface from the AFM tip. The experiments were carried out in PBS and deionized water for BSA- and dodecyl-tethered tips, respectively, at room temperature. More than 30 approach/retract cycles were performed for each polymer surface collected from at least 5 positions on the sample.

RESULTS AND DISCUSSION

Synthesis of Organic/Inorganic Hybrid Star-Shaped Polymers. A series of organic/inorganic hybrid star-shaped polymers (SPP#, where # is wt% of the PEGMA unit in the polymers) were synthesized via atom transfer radical polymerization (ATRP) using PEGMA and MA-POSS as monomers and octafunctional silsesquioxane (OBPS) as the initiator (Scheme 1). Star-shaped polymers with PEGMA and MMA monomeric units (SPM#, where # is wt% of the PEGMA unit in the polymers) were also prepared as a control group to study the effect of POSS on the antifouling coating properties of the star-shaped polymers. To obtain well-defined star-shaped polymers with multiple arms (>4), it is important to choose a suitable multifunctional initiator that can efficiently initiate polymerization of the monomers (PEGMA, MA-POSS, and MMA). OBPS has been demonstrated to be an efficient initiator for ATRP of methacryl monomers.[39] Additionally, MA-POSS,[41] MMA,[39] and PEGMA[42] monomers are compatible with ATRP.

Table 1 shows the results of the synthesis of SPPs and SPMs from different feed ratios of monomers such as PEGMA, MA-POSS, and MMA via ATRP. The monomer compositions were determined from ^{1}H NMR spectra of the polymers (Figure S1, Supporting Information). To use the polymers as antifouling coating materials for water treatment membranes, the solubility of the star-shaped polymers in water was controlled by incorporating different amounts of hydrophobic segments (P(MA-POSS) for SPPs and PMMA for SPMs) in the structures. We intentionally prepared SPPs with smaller MA-POSS content and SPMs with relatively larger MMA content because SPP and SPM were insoluble in water when the MA-POSS and MMA contents were larger than 13 and 54 wt %, respectively; the contents of MA-POSS in SPPs and of MMA in SPMs were from 0 to 43 wt % and from 31 to 74 wt %, respectively. Therefore, star-shaped antifouling coating polymers with stability in water were prepared by copolymerizing hydrophobic monomers such as MA-POSS or MMA with hydrophilic PEGMA, in which a much smaller amount of MA-POSS than that of MMA was used, because MA-POSS is obviously much more hydrophobic than MMA.[34]

The absolute and relative molecular weights of the star-shaped polymers were obtained by GPC using multiangle laser light scattering (MALLS) detector and refractive index (RI) detector, respectively. The relative molecular weights of the polymers obtained by the RI detector were much smaller than the corresponding absolute molecular weights obtained by MALLS detector. This was a result of the smaller hydrodynamic volume of the star-shaped polymers than that of the linear polymers when they have the same absolute molecular weight.[43] Additionally, THF is a good solvent for P(MA-POSS) and PMMA, but it is a relatively poor solvent for PPEGMA.[44] Therefore, the polymers with a larger content of PEGMA moieties displayed larger differences between their absolute and

Table 2. XPS Elemental Composition (in at %) of the Surfaces of SPP74- and SPM46-Coated Membranes, and Bare PSf Membrane

	C 1s								
sample	C−C C−Si	C−O	C═O	O 1s	Si 2p	S 2p	O 1s $_{PEGMA}$ [a] measured	O 1s $_{PEGMA}$ [b] theoretical	Si $_{POSS}$/O $_{PEGMA}$
PSf	58.26	26.95		12.85		1.94			
SPP74	33.90	30.25	4.34	26.50	5.01		17.68	24.42	0.28
SPM46	29.86	33.09	8.00	27.86	1.19		13.70	14.36	0.09

[a]Calculated from XPS elemental composition of the polymer-coated membrane surfaces. [b]Calculated from monomer composition and absolute molecular weight of the polymers.

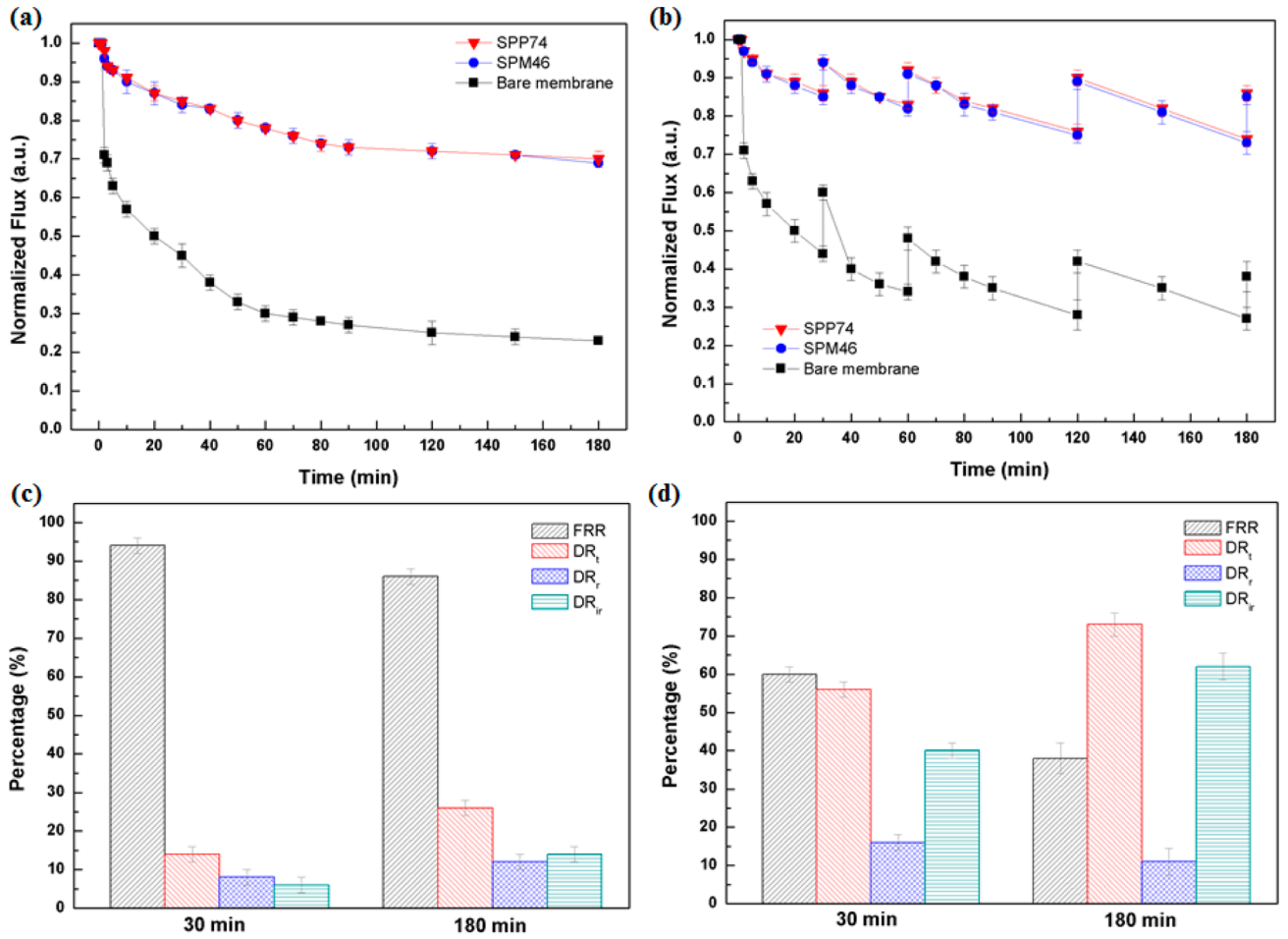

Figure 1. Time dependence of water permeation flux variations during membrane filtration: (a) flux behavior during BSA solution filtration and (b) flux behavior after cleaning with H_2O at 30, 60, 120, and 180 min, and summary of corresponding flux property values (flux-recovery ratio (FRR), total flux-decline ratio (DR_t), reversible flux-decline ratio (DR_r), and irreversible flux-decline ratio (DR_{ir})) of (c) SPP74-coated membrane and (d) bare PSf membrane.

relative molecular weights. The small polydispersity index values indicate that all polymers prepared using the ATRP technique in this study had a more or less uniform size distribution.

Preparation of Fouling-Resistant Membranes. PSf ultrafiltration membrane was used as the supporting membrane for surface modification and membrane fouling analysis, as it is widely used in separation processes, is commercially available, and is chemically inert.[11] Uniform and reproducible antifouling coating layers on the PSf membrane were prepared by spin-coating method. Methanol (MeOH) was used as the coating solvent, as other commonly used organic solvents such as acetone, THF, $CHCl_3$, DMF, and DMAc demaged the PSf membrane surface during the coating process. PSf is soluble or partially soluble in these solvents. Among the series of prepared polymers, SPP74 and SPM46 were chosen as antifouling coating materials, as they are insoluble in water but soluble in MeOH. By varying the polymer concentration of the coating solution, the thickness of the coating layer and the pure water flux of the membranes were controlled. When spin-coated using 1 wt % coating solutions, the polymer-coated membranes showed only small decreases in pure water flux compared with the pure water flux (530 $L(m^2h)^{-1}$, LMH) of a bare PSf membrane; 480 LMH (9.4% reduction) and 490 LMH (7.5% reduction) for SPP74- and SPM46-coated membranes, respectively. This decrease in flux was attributed to the decrease in pore sizes on the membrane surfaces after coating (see Figure S2 in the Supporting Information).[11,16] Although

dx.doi.org/10.1021/am301538h | ACS Appl. Mater. Interfaces 2012, 4, 5898−5906

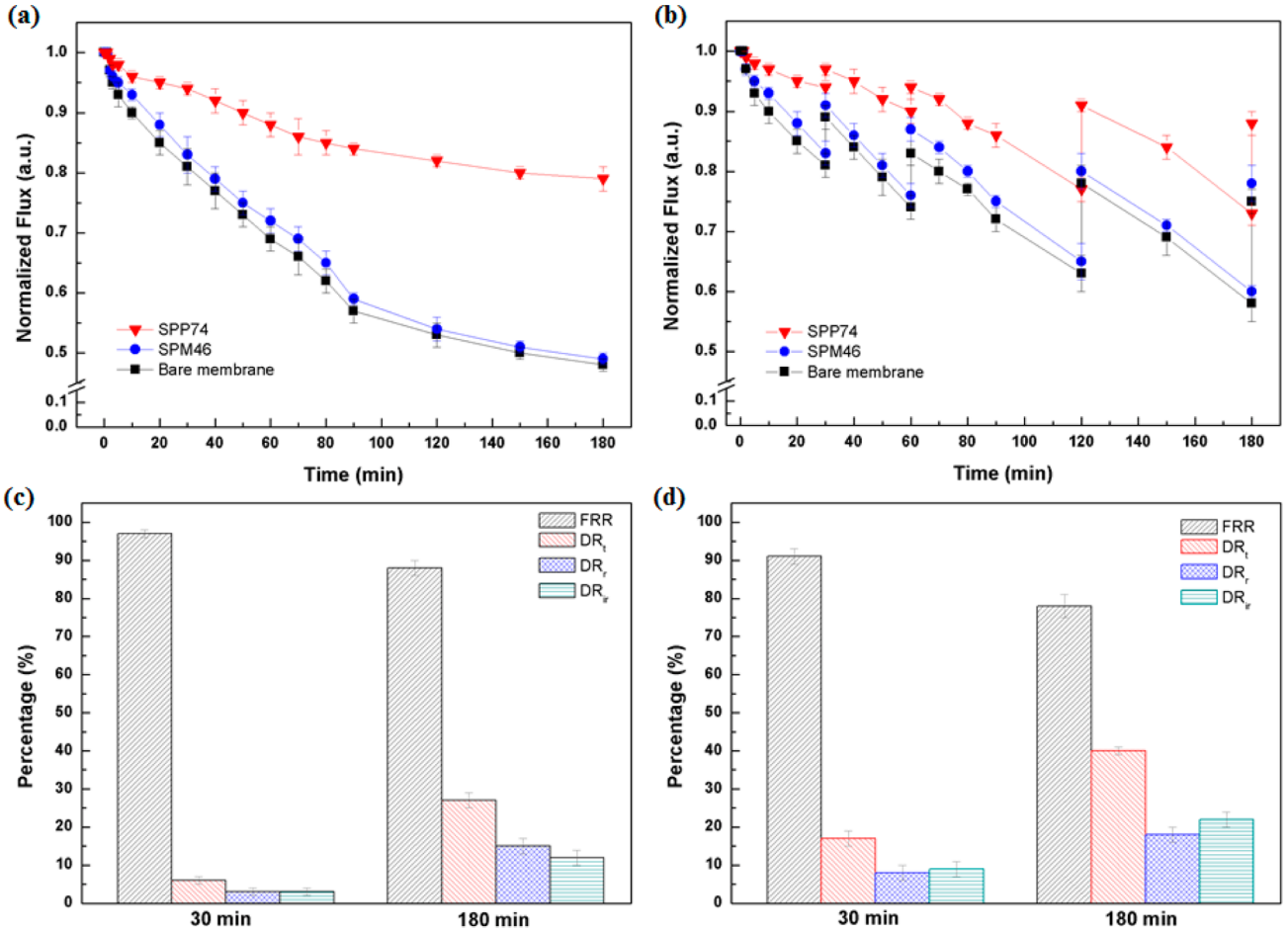

Figure 2. Time dependence of water permeation flux variations during membrane filtration: (a) flux behavior during oil/water emulsion filtration and (b) flux behavior after cleaning with H_2O at 30, 60, 120, and 180 min, and summary of corresponding flux property values (FRR, DR_t, DR_r, and DR_{ir}) of (c) SPP74- and (d) SPM46-coated membranes.

SPP87 was also used as a coating material, the water permeation flux and surface properties of the SPP87-coated membrane are not included in this study, because they were found to be quite similar with those of SPP74-coated membrane (see Table S1 and S2 in the Supporting Information). Therefore, the discussion in this manuscript focuses on the differences between the SPP74- and SPM46-coated membranes.

The surface elemental compositions of the polymer-coated and bare PSf membranes were characterized by XPS analysis (Table 2). The oxygen content increased upon addition of the polymer coatings to the membrane surfaces. Additionally, the S 2p peak observed for the bare PSf membrane did not appear in the star-shaped polymer-coated membranes. To further understand the chemical compositions of the polymer-coated membrane surfaces, we calculated the oxygen content originating from PEGMA moieties (O 1s $_{PEGMA}$ measured) in the polymers using the XPS elemental composition of the surfaces (Figure S3 and the detailed calculation, Supporting Information). The membrane surface coated with SPP74 had a larger O 1s $_{PEGMA}$ value than that coated with SPM46, although the total oxygen content (O 1s) of both membranes was similar. This could be ascribed to the larger content of PEGMA moieties in SPP74 than that in SPM46 (monomer composition in Table 1 and O 1s $_{PEGMA}$ theoretical in Table 2). The difference between the measured and theoretical O 1s $_{PEGMA}$ values indicates that the surfaces were enriched by hydrophobic segments such as P(MA-POSS) or PMMA than the hydrophilic PPEGMA segments. It is well-known that the hydrophobic moieties in the polymer tend to be located on the surface−air part rather than inside the polymer films.[45] Silicon content (i.e., POSS) and Si_{POSS}/O_{PEGMA} values were larger for the SPP74-coated membrane surface than the SPM46-coated surface, because SPP74 contained a larger amount of POSS than SPM46. Thus, the XPS result indicates that the SPP74-coated membrane had larger contents of both hydrophobic POSS and hydrophilic PEG segments than the SPM46-coated membrane.

Fouling Resistance and Flux-Recovery Ability. Dead-end membrane filtrations were performed to evaluate fouling resistance and flux-recovery ability of the membranes using bovine serum albumin (BSA) as a model biofoulant and vacuum pump oil as a model oil-foulant. Time-dependent, normalized permeation flux variations in the star-shaped polymer-coated membranes and the bare PSf membrane using BSA solution are shown in Figure 1a. The bare PSf membrane showed a larger flux decrease than the star-shaped polymer-coated membranes, possibly because of the favorable interactions between the PSf and BSA.[46] In contrast, larger steady-state flux values were observed in the membranes coated by the star-shaped polymers (SPP74 and SPM46) with the PEG moieties, because the hydrophilic PEG moieties have biofouling resistance.[47] The flux-decline ratio of the SPP74-

dx.doi.org/10.1021/am301538h | ACS Appl. Mater. Interfaces 2012, 4, 5898−5906

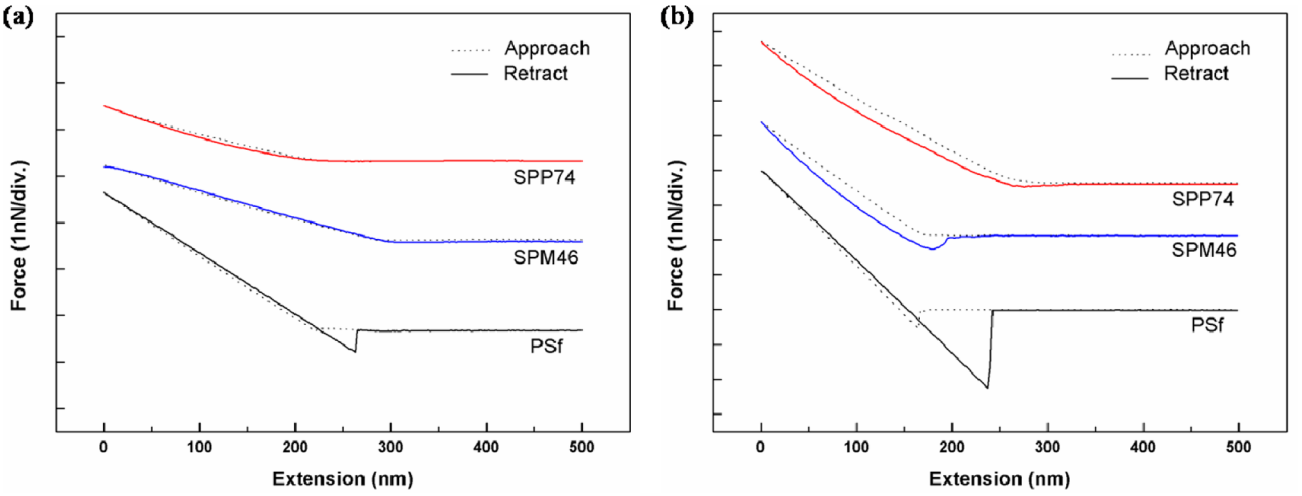

Figure 3. Force–extension curves recorded with (a) BSA- and (b) dodecyl-tethered AFM tips against SPP74, SPM46, and PSf surfaces coated on silicon wafer.

coated membrane was close to that of the SPM46-coated membrane and was about one-third compared with that of the bare PSf membrane (Figure 1a). Upon reaching a steady-state after 180 min of dead-end filtration, flux-decline ratios (DR), which were calculated from DR = (1 − normalized flux) × 100%, of the SPP74-coated and bare PSf membranes were 30% and 77%, respectively.

Figure 1b shows flux-recovery abilities of the star-shaped polymer-coated membranes and the PSf membrane. At 30, 60, 120, and 180 min after the initial feed of the BSA solution, the membranes were cleaned with deionized water for 10 min, and the water fluxes of the cleaned membranes were measured again. Flux-recovery ability of the membranes was evaluated by employing several parameters, including flux-recovery ratio (FRR), total flux-decline ratio (DR_t), reversible flux-decline ratio (DR_r), and irreversible flux-decline ratio (DR_{ir}), as summarized in panels c and d in Figure 1 (see the details of the calculation, Supporting Information). The FRR values of the PSf membrane were 60 and 38% at 30 and 180 min, respectively, and those of the SPP74-coated membrane were 94 and 86% at 30 and 180 min, respectively, indicating that the flux-recovery ability of the SPP74-coated membrane was much better than that of the bare PSf membrane. The SPP74-coated membrane also showed better performance in terms of flux-decline ratios than the PSf membrane. The DR_{ir} of the bare PSf membrane was much larger than the DR_r, whereas DR_{ir} of the SPP74-coated membrane was close to DR_r.

Oil-fouling resistance and flux-recovery ability of the membranes were also characterized from dead-end filtrations using an oil/water emulsion as shown in Figure 2. The SPM46-coated and bare PSf membranes showed larger flux decreases than the SPP74-coated membrane. Upon reaching a steady-state after 180 min of dead-end filtration, flux-decline ratios of the SPP74-coated and SPM46-coated membranes were 21% and 51%, respectively (Figure 2a). Although the SPM46-coated membrane contained larger hydrophilic moieties than the bare PSf membrane (Table 2), its oil-fouling resistance was close to that of the bare membrane.

The flux-recovery abilities of the star-shaped polymer-coated membranes and PSf membrane in oil/water emulsion filtration are shown in Figure 2b–d. The membranes were cleaned with deionized water for 10 min at 30, 60, 120, and 180 min after the initial feed of the oil/water emulsion, after which the water fluxes of the cleaned membranes were measured again. The flux-recovery ability of SPP74-coated membrane was much better than that of the SPM46-coated membrane and bare PSf membrane, although the SPM46-coated membrane exhibited slightly better performance than the bare PSf membrane. The FRR values of the SPM46-coated membrane were 91 and 78% at 30 and 180 min, respectively, and those of the SPP74-coated membrane were 97 and 88% at 30 and 180 min, respectively. The SPP74-coated membrane also showed better performance in terms of flux-decline ratios than the SPM46-coated membrane. The DR_{ir} of the SPM46-coated membrane was slightly larger than the DR_r, whereas DR_{ir} of the SPP74-coated membrane were almost identical to or even lower than DR_r. Therefore, it is quite clear that the membrane surface with a larger content of hydrophobic POSS and hydrophilic PEG moieties had better antifouling properties against both bio- and oil-foulants.

Surface Properties and Fouling Resistance Mechanisms. The surface properties of the membranes were studied to understand the underlying mechanisms of fouling resistance and flux-recovery ability of the membranes. At first, sessile drop water contact angles were measured to estimate the relative hydrophilicity of the membranes. The bare PSf membrane showed a larger contact angle value than SPP74- and SPM46-coated membranes (see Figure S4 in the Supporting Information). When the water contact time increased, the contact angles on PSf membrane remained almost stable, whereas those on the star-shaped polymer-coated membranes decreased gradually with time. The time-dependent wetting behavior of the star-shaped polymer-coated membranes should have originated from the hydrophilic porous surfaces as reported previously.[9,49] The decrease in the water contact angle on the SPP74-coated membrane was slightly larger than that on the SPM46-coated membrane, indicating that SPP74 is more hydrophilic than SPM46, although the SPP74 has a larger amount of hydrophobic POSS moieties than SPM46. This could be ascribed to the fact that the SPP74-coated membrane contained a larger amount of hydrophilic PEG moieties as well as the hydrophobic POSS moieties than SPM46-coated membrane as estimated by the XPS results in Table 2. Although there are only few works in which membrane fouling

dx.doi.org/10.1021/am301538h | ACS Appl. Mater. Interfaces 2012, 4, 5898–5906

is directly correlated to the hydrophilicity of the membrane surface, it is generally assumed that an increase in hydrophilicity on membrane surfaces by PEG increases the fouling resistance.[6]

Fouling is governed by the interaction between the foulant and the membrane surface. Thus, the adhesion force of proteins against the material surface is an important parameter that allows a direct assessment of protein adsorption behaviors on the surfaces. Previous results by us and others have also shown that the magnitude of the adhesion force correlates well with the fouling propensity of membranes and polymer-coated surfaces in the presence of organic foulants.[7,13,38,48] Figure 3a shows typical force−extension curves when a BSA-tethered AFM tip interacts with polymer films on a silicon wafer in phosphate buffer solution. As uneven membrane surfaces containing pores can affect the measurement of interaction forces between polymer films and the BSA-tethered AFM tip, flat polymer surfaces, prepared by spin-coating on silicon wafer, were used to obtain force−extension curves. Large pull-off forces were detected for PSf compared with the star-shaped polymers, as indicated by the large negative values (0.39 ± 0.16 nN). In contrast, no measurable adhesion forces were detected from the star-shaped polymer-coated surfaces. Therefore, the very small interactive forces between the star-shaped polymers and proteins should provide the excellent biofouling resistance for the surface of the star-shaped polymer-coated membranes.

In comparison to the star-shaped polymer-coated membranes, the bare PSf membrane exhibited a significant flux-decline at the initial filtration stage, resulting in about three times larger flux-decline after 180 min of filtration than that of the membranes coated with SPP74 and SPM46 having PEG moieties (Figure 1a). PEG has been recognized as a material uniquely suited for preventing the adsorption of proteins and bacteria.[6,37,47] As the PEG has neutrally charged chemical structure with no dissociable functional group, the interaction between PEG and BSA is not electrostatic but another nonspecific interaction, namely steric repulsion.[8,14] In addition, an energetic barrier for the interaction between PEG and BSA in an aqueous condition is created by favorable water−PEG interactions.[47] It is also known that the PEG is flexible because of its ether linkages and has a large excluded volume in water, tending to repel the BSA.[8,14,37,47] These properties of PEG in the star-shaped polymer coatings give the energetic and steric-entropic barrier to the adhesion of BSA on the membrane surface. Therefore, the SPP74 and SPM46 coating layers on the membranes should reduce the initial adhesion of BSA to the membrane surface and the removal of the fouled BSA was more effective, resulting in reduced flux-declines and enhanced flux-recovery abilities.

The oleophobicity of the membrane surfaces was studied from the decane captive bubble contact angle measurement (see Figure S5 in the Supporting Information). In comparison to sessile water drops, the decane captive bubbles were stable during measurement; almost no changes were observed in the contact angle with time. A bare PSf membrane showed the largest contact angle value (78.6 ± 2.4 °), indicating that it has the most oleophilic surface. Additionally, the contact angle of the SPP74-coated membrane (59.7 ± 1.5°) was smaller than that of the SPM46-coated membrane (64.5 ± 2.8 °), clearly indicating that the SPP74-coated membrane has more oleophobic surface in a water environment than the SPM46-coated membrane. Interaction forces between a dodecyl-tethered AFM tip and polymer films on silicon wafer in deionized water were also analyzed as shown in Figure 3b. Larger interaction forces (2.33 ± 0.06 nN) were detected for PSf, whereas relatively smaller forces were detected from the star-shaped polymer-coated surfaces. Moreover, the interaction forces between the dodecyl-tethered AFM tip and SPP74 surface (0.09 ± 0.05 nN) were found to be smaller than that between the tip and SPM46 surface (0.40 ± 0.10 nN). Thus, the interaction forces are consistent with the relative oleophobicity of the membranes analyzed by the decane captive bubble contact angles. Hydrophilic PEG groups are known to increase the antioil-fouling properties of the surfaces by decreasing the hydrophobic interaction with oils.[16,17,20] Simultaneously, POSS has also been applied as a surface modifier to enhance the oleophobicity.[30−33] Therefore, the SPP74 surface containing both larger amounts of PEG and POSS moieties exhibited the most oleophobic surface.

Although the oleophobicity of the membranes was correlated with their flux behaviors, the oil-fouling resistant properties of the membranes could not be fully elucidated from the oleophobicity results of the decane captive bubble contact angle and interaction force measurements. The hydrophilic SPM46-coated membrane was more oleophobic than PSf membrane as estimated by the decane captive bubble contact angle values, whereas the flux-declines measured from oil/water emulsion filtration using the SPM46-coated and PSf membranes were not much different as shown in Figure 2a. In contrast, the amphiphilic SPP74-coated membrane showed much higher oil-fouling resistance and flux-recovery abilities than the bare membrane. This could be ascribed to the different fouling behavior of oils compared to that of biofoulants. When the oil/water emulsion is applied to membrane filtration, the poorly stabilized oil drops tend to adhere to the membrane surface and reorganize themselves, and they even coalesce with each other and spread to form a continuous oil-fouling film on the membrane surfaces.[20,21,42,50] The hydrophilic SPM46-coating layer could weaken the hydrophobic interactions between the oil droplets and the membrane surface, resulting in a larger flux-recovery than the bare PSf membrane (Figure 2b), whereas it could not effectively prevent the formation of the oil-fouling film caused by coalescence and spreading of oil droplets on the membrane surfaces.[21] We also believe that the quite large quantity of MMA monomeric units on the SPM46-coated membrane surface can increase the interaction with the oil spreads, which decreases the flux of the oil/water emulsion. Solubility parameter has been used to indicate the polarity of a polymer. The solubility parameters of PMMA and PSf are close in the range of 18−21 $(MPa)^{1/2}$,[51] which might produce a similar interactive forces between these polymers and oil spreads.

The amphiphilic SPP74-coated membrane also showed higher oil-fouling resistance than the membrane coated with solely hydrophobic star-shaped P(MA-POSS) (SP) in the oil/water emulsion filtration; the water permeation flux values of the SPP74-coated membrane are larger than the SP-coated membrane, and the flux-recovery ability of the SPP74-coated membrane is also better than that of the SP-coated one (see Figure S6 in the Supporting Information). It was reported by others that oil droplets show nonwetting behavior (larger oil contact angle values) on the surfaces of low surface energy materials such as fluoropolymers or POSS moieties at the solid-air-oil interface.[30−34] On the contrary, the oil droplets on the same low surface energy materials in water (i.e., solid-water-oil interface) shows more oleophilic behavior; the oil droplets favorably adhere on them showing smaller oil contact angle

values.[52] Therefore, we believe that the amphiphilicity of the SPP coatings with a larger amount of both hydrophilic PEG and hydrophobic POSS moieties is very important to effectively prevent the oil-fouling during oil/water emulsion filtration.

Structural models demonstrating the dual effective SPP-coating layers on membrane surfaces for bio- and oil-fouling resistance are described in Scheme 2. As confirmed by the XPS

Scheme 2. Schematic Illustration of Fouling-Resistant Surfaces of (a) SPP- and (b) SPM-Coated Membranes

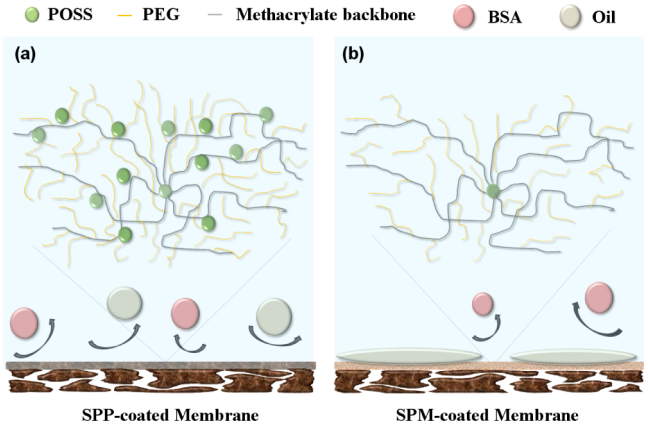

results (Table 2), the SPP-coated membrane had a large quantity of both hydrophobic POSS and hydrophilic PEG moieties on the surface. In contrast, the SPM-coated membrane has a smaller quantity of POSS and PEG moieties but a larger quantity of medium polar MMA moieties. In an aqueous environment, the hydrophilic PEG moieties on a membrane surface are hydrated and they can repel the protein and oil because they provide energetic and steric-entropic barrier to the adhesion of the foulants.[4,8,14,47] Meanwhile, the hydrophobic POSS moieties on a membrane surface could prevent the formation of a continuous oil-fouling film originating from the coalescence and spreading of oil droplets.[21,22] Therefore, the smaller interaction forces with protein and the higher oil-repellency of the membranes were achieved using the star-shaped polymers with the organic/inorganic hybrid structures.

CONCLUSION

Amphiphilic organic/inorganic hybrid star-shaped polymer (SPP)-coated membranes demonstrated noticeably improved bio- and oil-fouling resistant properties, as compared with the bare PSf ultrafiltration membrane. Moreover, the SPP surfaces exhibited better oil-fouling resistance and flux-recovery ability when compared with the SPM46 surface containing PEGMA and MMA moieties, whereas their biofouling resistance and flux-recovery ability were found to be close to those of the SPM46 surface. These interesting properties of the SPP surfaces could be ascribed to the larger amounts of both hydrophilic PEGMA and hydrophobic POSS moieties on the surfaces. The simultaneous enrichment of hydrophilic and hydrophobic segments on the membrane surfaces decreased interactions with protein and oil, resulting in the enhanced fouling resistance and flux-recovery ability of the membranes. We believe that this dual effective antifouling coating material could be a good candidate for use in membrane surface modification.

ASSOCIATED CONTENT

Supporting Information

Additional tables and figures: water permeation flux property values, surface composition, and properties of SPP87-coated membrane or silicon wafer (Table S1 and S2), ^{1}H NMR spectra (Figure S1) and the detailed calculation of monomer composition of the star-shaped polymers, SEM micrographs (Figure S2), XPS C 1s core level spectra (Figure S3), the detailed calculating method of O 1s $_{PEGMA}$ value, time-dependent sessile drop water contact angles (Figure S4) and decane captive bubble contact angles (Figure S5) of the membrane surfaces, and water permeation flux variations of SP-coated membrane during oil/water emulsion filtration (Figure S6). This material is available free of charge via the Internet at http://pubs.acs.org.

AUTHOR INFORMATION

Corresponding Author

*E-mail: jongchan@snu.ac.kr (J.-C.L.); denis.kang@samsung.com (H.K.). Phone: +82 2 880 7070 (J.-C.L.); +82 31 280 9255 (H.K.). Fax: +82 2 888 1604 (J.-C.L.); +82 31 280 9359 (H.K.).

Author Contributions

†These authors contributed equally.

Notes

The authors declare no competing financial interest.

ACKNOWLEDGMENTS

This research was supported by a grant from the Fundamental R&D Program for Technology of World Premier Materials funded by the Ministry of Knowledge Economy, Republic of Korea.

REFERENCES

(1) Shannon, M. A.; Bohn, P. W.; Elimelech, M.; Georgiadis, J. G.; Marinas, B. J.; Mayes, A. M. *Nature* **2008**, *452*, 301−310.
(2) Freeman, B. D.; Pinnau, I. In *Advanced Materials for Membrane Separations*; American Chemical Society: Washington, D.C., 2004, Vol. *876*, pp 1−23.
(3) Goosen, M. F. A.; Sablani, S. S.; Al-Hinai, H.; Al-Obeidani, S.; Al-Belushi, R.; Jackson, D. *Sep. Sci. Technol.* **2005**, *39*, 2261−2297.
(4) Hilal, N.; Ogunbiyi, O. O.; Miles, N. J.; Nigmatullin, R. *Sep. Sci. Technol.* **2005**, *40*, 1957−2005.
(5) Mansouri, J.; Harrisson, S.; Chen, V. *J. Mater. Chem.* **2010**, *20*, 4567−4586.
(6) Rana, D.; Matsuura, T. *Chem. Rev.* **2010**, *110*, 2448−2471.
(7) Asatekin, A.; Kang, S.; Elimelech, M.; Mayes, A. M. *J. Membr. Sci.* **2007**, *298*, 136−146.
(8) Kang, S.; Asatekin, A.; Mayes, A. M.; Elimelech, M. *J. Membr. Sci.* **2007**, *296*, 42−50.
(9) Zhao, Y.-H.; Zhu, B.-K.; Kong, L.; Xu, Y.-Y. *Langmuir* **2007**, *23*, 5779−5786.
(10) Singh, A. K.; Prakash, S.; Kulshrestha, V.; Shahi, V. K. *ACS Appl. Mater. Interfaces* **2012**, *4*, 1683−1692.
(11) Hyun, J.; Jang, H.; Kim, K.; Na, K.; Tak, T. *J. Membr. Sci.* **2006**, *282*, 52−59.
(12) McCloskey, B. D.; Park, H. B.; Ju, H.; Rowe, B. W.; Miller, D. J.; Chun, B. J.; Kin, K.; Freeman, B. D. *Polymer* **2010**, *51*, 3472−3485.
(13) Asatekin, A.; Menniti, A.; Kang, S.; Elimelech, M.; Morgenroth, E.; Mayes, A. M. *J. Membr. Sci.* **2006**, *285*, 81−89.
(14) Adout, A.; Kang, S.; Asatekin, A.; Mayes, A. M.; Elimelech, M. *Environ. Sci. Technol.* **2010**, *44*, 2406−2411.
(15) Cheryan, M.; Rajagopalan, N. *J. Membr. Sci.* **1998**, *151*, 13−28.
(16) Ju, H.; McCloskey, B. D.; Sagle, A. C.; Wu, Y.-H.; Kusuma, V. A.; Freeman, B. D. *J. Membr. Sci.* **2008**, *307*, 260−267.

(17) Asatekin, A.; Mayes, A. M. *Environ. Sci. Technol.* **2009**, *43*, 4487−4492.
(18) Nunes, S. P.; Sforça, M. L.; Peinemann, K.-V. *J. Membr. Sci.* **1995**, *106*, 49−56.
(19) Chu, L.-Y.; Wang, S.; Chen, W.-M. *Macromol. Chem. Phys.* **2005**, *206*, 1934−1940.
(20) Chen, W.; Peng, J.; Su, Y.; Zheng, L.; Wang, L.; Jiang, Z. *Sep. Purif. Technol.* **2009**, *66*, 591−597.
(21) Chen, W.; Su, Y.; Peng, J.; Dong, Y.; Zhao, X.; Jiang, Z. *Adv. Funct. Mater.* **2011**, *21*, 191−198.
(22) Chen, W.; Su, Y.; Peng, J.; Zhao, X.; Jiang, Z.; Dong, Y.; Zhang, Y.; Liang, Y.; Liu, J. *Environ. Sci. Technol.* **2011**, *45*, 6545−6552.
(23) Wang, F.; Lu, X.; He, C. *J. Mater. Chem.* **2011**, *21*, 2775−2782.
(24) Ryu, H.-S.; Kim, D.-G.; Lee, J.-C. *Polymer* **2010**, *51*, 2296−2304.
(25) Kopesky, E. T.; Haddad, T. S.; Cohen, R. E.; McKinley, G. H. *Macromolecules* **2004**, *37*, 8992−9004.
(26) Dong, F.; Ha, C.-S. *Macromol. Res.* **2012**, *20*, 335−343.
(27) Ryu, H.-S.; Kim, D.-G.; Lee, J.-C. *Macromol. Res.* **2010**, *18*, 1021−1029.
(28) Meuler, A. J.; Chhatre, S. S.; Nieves, A. R.; Mabry, J. M.; Cohen, R. E.; McKinley, G. H. *Soft Matter* **2011**, *7*, 10122−10134.
(29) Iacono, S. T.; Budy, S. M.; Smith, D. W.; Mabry, J. M. *J. Mater. Chem.* **2010**, *20*, 2979−2984.
(30) Tuteja, A.; Choi, W.; Ma, M.; Mabry, J. M.; Mazzella, S. A.; Rutledge, G. C.; McKinley, G. H.; Cohen, R. E. *Science* **2007**, *318*, 1618−1622.
(31) Gao, Y.; He, C.; Qing, F.-L. *J. Polym. Sci., Polym. Chem.* **2011**, *49*, 5152−5161.
(32) Jerman, I.; Koželj, M.; Orel, B. *Sol. Energy Mater. Sol. Cells* **2010**, *94*, 232−245.
(33) Chhatre, S. S.; Tuteja, A.; Choi, W.; Revaux, A. l.; Smith, D.; Mabry, J. M.; McKinley, G. H.; Cohen, R. E. *Langmuir* **2009**, *25*, 13625−13632.
(34) Gao, Y.; He, C.; Huang, Y.; Qing, F.-L. *Polymer* **2010**, *51*, 5997−6004.
(35) Allegra, G.; Ganazzoli, F. *Prog. Polym. Sci.* **1991**, *16*, 463−508.
(36) Inoue, K. *Prog. Polym. Sci.* **2000**, *25*, 453−571.
(37) Gasteier, P.; Reska, A.; Schulte, P.; Salber, J.; Offenhäusser, A.; Moeller, M.; Groll, J. *Macromol. Biosci.* **2007**, *7*, 1010−1023.
(38) Kim, D.-G.; Kang, H.; Han, S.; Lee, J.-C. *J. Mater. Chem.* **2012**, *22*, 8654−8661.
(39) Costa, R. O. R.; Vasconcelos, W. L.; Tamaki, R.; Laine, R. M. *Macromolecules* **2001**, *34*, 5398−5407.
(40) Cho, E. C.; Kim, D.-H.; Cho, K. *Langmuir* **2008**, *24*, 9974−9978.
(41) Pyun, J.; Matyjaszewski, K. *Macromolecules* **1999**, *33*, 217−220.
(42) Nabi, N.; Aimar, P.; Meireles, M. *J. Membr. Sci.* **2000**, *166*, 177−188.
(43) Matyjaszewski, K.; Miller, P. J.; Pyun, J.; Kickelbick, G.; Diamanti, S. *Macromolecules* **1999**, *32*, 6526−6535.
(44) Taton, D.; Cloutet, E.; Gnanou, Y. *Macromol. Chem. Phys.* **1998**, *199*, 2501−2510.
(45) Sohn, E.-H.; Ahn, J.; Kim, B. G.; Lee, J.-C. *Langmuir* **2010**, *27*, 1811−1820.
(46) Koehler, J. A.; Ulbricht, M.; Belfort, G. *Langmuir* **1997**, *13*, 4162−4171.
(47) Banerjee, I.; Pangule, R. C.; Kane, R. S. *Adv. Mater.* **2011**, *23*, 690−718.
(48) Weinman, C. J.; Gunari, N.; Krishnan, S.; Dong, R.; Paik, M. Y.; Sohn, K. E.; Walker, G. C.; Kramer, E. J.; Fischer, D. A.; Ober, C. K. *Soft Matter* **2010**, *6*, 3237−3243.
(49) Guo, H.; Ulbricht, M. *J. Membr. Sci.* **2011**, *372*, 331−339.
(50) Dresselhuis, D. M.; van Aken, G. A.; de Hoog, E. H. A.; Stuart, M. A. C. *Soft Matter* **2008**, *4*, 1079−1085.
(51) Brandrup, J.; Immergut, E. H.; Grulke, E. A.; Abe, A.; Bloch, D. R. In *Polymer Handbook*, 4th ed.; Wiley-Interscience: New York, 1999; Vol. 2, pp 675−714.
(52) Jung, Y. C.; Bhushan, B. *Langmuir* **2009**, *25*, 14165−14173.